STUDY OF THE WATER CLEANING PROCESS BY USING CFD-DEM METHOD
A Cace Study of Coarse Filter Material

by

Xin ZHANG[a,b], Zeming FU[c], Tianyu ZHOU[a], Jinjiang LIU[a], Min YANG[a], Xingxin NIE[a*], Huagen WU[c*], Ping CHENG[a*], Tong GUO[d], and Xiaoxin LUO[e*]

[a] School of Resources Engineering, Xi'an University of Architecture and Technology, Xi'an, China
[b] School of Environmental and Municipal Engineering, Xi'an University of Architecture and Technology, Xi'an, China
[c] School of Energy and Power Engineering, Xi'an Jiaotong University, Xi'an, China
[d] Zhashui Qintong Construction Co., Ltd., Shangluo, China
[e] Shaanxi Metallurgical Design and Research Institute Co., Ltd., Xi'an, China

Original scientific paper
https://doi.org/10.2298/TSCI230206088Z

In this paper, the CFD-DEM coupling method was utilized to study the water cleaning and regeneration process of fibrous filter material. The effects of cleaning flow rate, time and adhesion force on the particle removal process were simulated. The results showed that the particle removal rate had a diminishing marginal effect with the increasing of cleaning flow rate. More than 80% of the particles were removed in the initial period, and then tended to stabilize. The higher the flow rate, the shorter the time needed to achieve stability. For G4 filter material, the function between the particle removal rate and the cleaning flow rate and time was given, and the best cleaning flow rate was 1.2 m/s while the cleaning time was 30 seconds. The surface energy of the fibers plays a dominant role in the cleaning process, and the reduction 1/4 of the surface energy of the particles can effectively improve the cleaning and regeneration performance.

Key words: *fibrous filter, water cleaning, regeneration, CFD-DEM, fine particles*

Introduction

Atmospheric PM pollution has become a serious global problem, especially $PM_{2.5}$ [1]. Fiber filtration is the most effective way to control indoor $PM_{2.5}$ [2]. However, the deposition of particles on the surfaces and micropores of the fibrous filter material would lead to partial blockage of the air-flow and also increase the filtration resistance, which would increase energy consumption [3, 4]. When the air filter reaches its service life, the frequent replacement will cause material waste and increase usage cost. Improper disposal of used filters may also bring new environmental pollution [5]. Traditional fibrous filter material had poor degradability and may release particulate contaminants during disposal in landfills or incineration [6], such as polyethylene (PE) and polypropylene (PP). The cleaning and regeneration of fibrous filter material have received extensive attention in recent years.

* Corresponding authors, e-mail: niexingxin@xauat.edu.cn, hgwu@mail.xjtu.edu.cn, chengp_314@163.com

Water cleaning is a common convenient and low cost method for material recycling, and it is widely used in all walks of life. Some scholars also have carried out relevant experimental researches [7-9], such as the research on the cleaning effect of conventional coarse and medium efficiency filter material [7], the research on the cleaning effect of reverse water [8], the research on the cleaning time [9], and the filter bed design and methods of washing [10]. However, there is a lack of specific research on relevant parameters, as well as repeated and clear research. In addition, the type of water used for cleaning is also one of the indicators that determine the filter cleaning standard. The water quality will affect the residue of microorganisms and the content of bacteria [11, 12]. Some scholars have prepared a variety of washable fibrous filters in recent years, but there is still a lack of in-depth research on the effects of microscopic forces, flow characteristics and interface properties during cleaning [13]. There is a new type of high efficiency filter composed of the polytetrafluoroethylene and nylon fabrics at present, and the results showed that the removal efficiency has little change after five washing cycles, with high stability [14]. However, fiber filtration and cleaning are essentially a combined problem of fluid-solid two-phase flow in micron-sized pores with particle contact adhesion and detachment in theory. The particle-fluid interaction forces during water cleaning are complex, and the van der Waals force of micron-sized particles is very important [15]. Coupled computational fluid dynamics-discrete element method (CFD-DEM) is a multi-scale Eulerian-Lagrangian technique and has advantages for considering the influence of various forces on the particle motion state [16].

A 3-D model of the coarse filter material was designed to simulate the microscopic process of cleaning in this paper. The influences of cleaning flow rate, time and adhesion force on the particle removal process were discussed, and the change of particle kinetic behavior was revealed. This study provides new insight into the cleaning of fibrous filter material.

Methods

The flow of the fluid phase in the CFD model is determined by the volume-averaged Navier-Stokes and the continuity equation [17]:

$$\frac{\partial(\varepsilon\rho_f u_f)}{\partial t} + \nabla(\varepsilon\rho_f u_f u_f) = -\varepsilon\nabla p + \nabla(\varepsilon\tau_f) + \varepsilon\rho_f \mathrm{g} - S \tag{1}$$

$$\frac{\partial(\varepsilon\rho_f)}{\partial t} + \nabla(\varepsilon\rho_f u_f) = 0 \tag{2}$$

where ρ_f, τ_f, u_f are the density, stress tensor, and the velocity of the fluid, g, p, and ε – the gravitational acceleration, pressure, and porosity, and S – the momentum exchange between the fluid phase and the particulate phase.

The transition and rotational motion of each particle is expressed by Newton's second law in the DEM [18]:

$$m_i \frac{\partial x_i}{\partial t} = F_\mathrm{c} + F_\mathrm{nc} + F_\mathrm{d} + F_\mathrm{p} \tag{3}$$

$$I\frac{\partial_\omega}{\partial_\mathrm{t}} = M_T + M_R \tag{4}$$

where F_c is the contact force, F_nc – the non-contact force, F_d – the resistance of the fluid to the particle, F_p – the pressure gradient force, M_T – the torque due to tangential contact force, and M_R – the torque due to rolling friction.

The models of Hertz-Mindlin [19] and Johnson-Kendall-Roberts (JKR) contact model [20] are both used throughout this paper. In order to remove the deposited particles, sufficient removal force should be applied to overcome the adhesion between particles and fibers. The hydrodynamic force is the primary removal force that detached the deposited particles from the surfaces [21]. The Gidaspow model was used, which is the combination of the equations of Xie *et al.* [22].

Commercial software ANSYS FLUENT 19.0 and EDEM 2018 were used to conduct a coupled simulation in the Euler-Lagrange framework. To start the CFD-DEM coupling, the flow field is first calculated to converge in CFD. Then the flow information is transferred to the DEM and the interaction forces between the fluid and the particles are calculated to obtain information such as the velocity and position of the particles. Finally, the flow field is updated taking into account the effect of the particles and the simulation proceeds to the next time step.

Establishment of numerical model

The 3-D filter and computational domain

A typical laminar filter structure was used to simplify the model in this paper [23, 24]. It was based on the following assumptions: the filter material was laminar, all fibers were oriented horizontally and had the same fiber diameter, and the fibers were randomly interlaced. Washable fiber material generally had high mechanical strength and good chemical stability [25]. The structure was assumed to be constant in the simulation. The 3-D model was simplified to eight layers with a layer spacing of 15 μm and model thickness of 225 μm. The fiber diameter, porosity and fiber density were set according to G4 filter material and compared experimentally by dimensionless parameters. Table 1 shows the structural parameters of G4 filter material [26, 27].

Table 1. Parameters of G4 filter material

Grade	Fiber diameter [μm]	Porosity [%]	Thickness [mm]	Basis weight [gm^{-2}]	Density [kgm^{-3}]
G4	15	95.12	2	108.76	1380

The 3-D filter model and the computational domain were shown in fig. 1. Water flowed along the *z*-axis in the positive direction for cleaning, opposite to the direction of air filtration. Non-slip boundary condition was taken to the fiber surfaces. The water flow inlet boundary was imposed velocity inlet, and the outlet boundary condition was imposed pressure outlet.

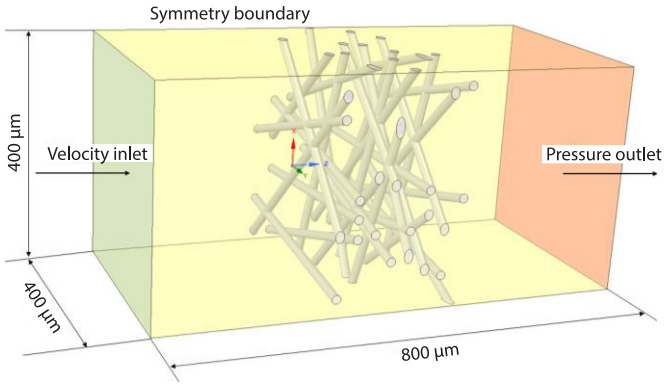

Figure 1. Computational domain and boundary conditions

The standard k-ε model was chosen to calculate the two-phase flowed field within the fibrous filter material [28]. The relevant parameters settings were shown in tab. 2.

Table 2. Parameters applied to the simulation

Parameters	Particle	Fiber
Density [kgm^{-3}]	2000	1380
Poisson's ratio	0.25	0.21
Shear modulus [Pa]	$2.2 \cdot 10^8$	$3 \cdot 10^{10}$
Coefficient of restitution	0.5	0.3
Coefficient of static friction	0.2	0.2
Coefficient of rolling friction	0.1	0.1
Surface energy [Jm^{-2}]	0.1~0.5	0.05~0.5

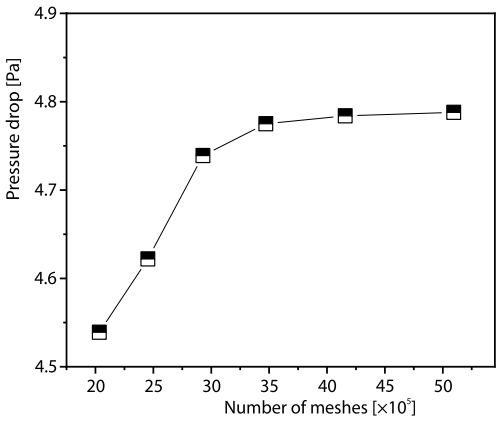

Figure 2. Mesh independence tested

Mesh

The arrangement of fibers in the computational domain was complicated and irregular. So an unstructured tetrahedral grid was performed. The particle motion and the flow field near the fibers were more complex and require mesh encryption. Mesh independence should be verified to exclude the influence of the mesh number on the simulation results. The initial filtration resistance of the 3-D filter was simulated at a wind speed of 1.0 m/s. The variation of the filtration resistance of the increasing of the number of grids was showed in fig. 2. The initial filtration resistance starts to level off when the number of grids is about 3.47 million. The continued increased of grids have no significant effect on the calculation results, and the grid size near the fibers is 8 μm in this number of grids.

Experimental systems and model verification

The schematic diagram of the experimental test set-up was shown in fig. 3. The experimental set-up was built according to China's national standard (GB/T 14295-2019) [29]. The distribution of measuring points was compiled according to China's national standard (GB50019-2015) [29]. An HD2114P.0 Portable Micromanometer was used to measure filter resistance. The measuring accuracy is ±(2% reading + 0.1 m/s), and the pressure range is ±0.4% F.S. An HD37AB1347 Indoor Air Quality Monitor was used to measure the veloci-

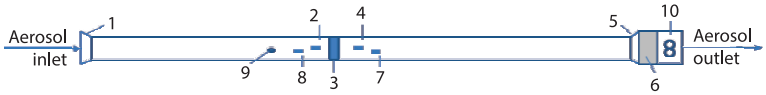

Figure 3. Diagram of filter performance test bench: *1 – current collector, 2 – upstream static pressure probe, 3 – tested filter, 4 – downstream static pressure probe, 5 – expanding tube, 6 – soft connection, 7 – downstream sampling head, 8 – upstream sampling head, 9 – wind speed hole, and 10 – axial fan*

ty. The measuring accuracy range is ±3%. A GRIMM1.109 Portable Aerosol Spectrometer was used to measure concentrated particles before and after the air filters were applied. The upper limit of counting concentration was 2000000 P per L. The particles ranging from 0.25-32 μm in diameter could be separated into 31 channels. The repeatability was 5%. The particle size distribution of the experimental dust was shown in fig. 4. The particle sizes were shown with an average value of about 2.5 μm.

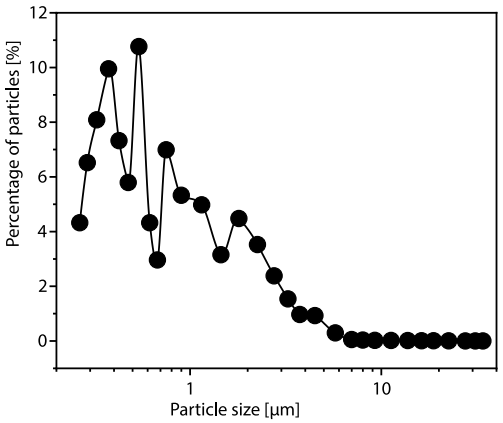

Figure 4. Distribution of particle sizes

Five pieces of the same material of G4 filter by using the dust were loaded to the same resistance at the filtration velocity of 1.0 m/s. The cleaning time was 10 seconds, 20 seconds, 30 seconds, 40 seconds, and 50 seconds at the water flow rate of 1.2 m/s, respectively. The removal rate was calculated by weighing the fibrous filter material before and after cleaning, with repeated five times.

The dimensionless resistance was used to compare and verify. The air-flow through the fibrous filter material is laminar, and the resistance was expressed as Darcy's law [30]:

$$\frac{\Delta p}{H} = f(\alpha)\frac{\mu V}{d_f^2} \tag{5}$$

where $f(\alpha)$ is the dimensionless resistance, μ – the dynamic viscosity of the air, d_f – the fiber diameter, and H – the filter thickness.

The comparison of the dimensionless resistance between CFD-DEM simulation and G4 experimental results was shown in fig. 5(a). The slope value of the linear fit is , and the relative deviation is 3.23%. The cleaning time of the simulation and experiment was normalized. The comparison of the particle removal rate between simulation and experiments with the trend of cleaning time under 1.2 m/s was shown in fig. 5(b). The removal rate in the simulation was statistically calculated for the number of deposited particles before and after cleaning. The variation trends of the simulated and experimental results were in line, with an average deviation of 3.55%. In a word, the established 3-D filter and the CFD-DEM coupling method are accurate and credible.

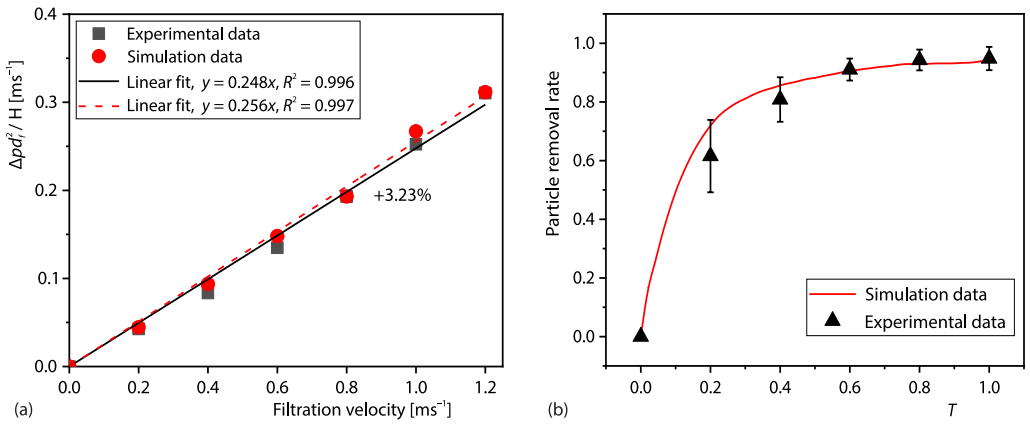

Figure 5. Results comparison of initial non-dimensional resistance (a) and particle removal rate between the experimental test and simulation (b)

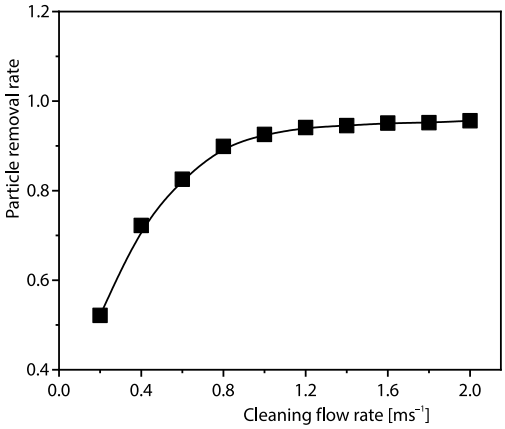

Figure 6. Effect of cleaning flow rate of final particle removal rate

Results and discussion

Effect of the cleaning flow rate

The particles are subjected to a consequent change in flow traction at different cleaning flow rates, which will affect the detachment and movement of the particles from the fiber. The change of the final removal rate of particles with the cleaning flow rate after cleaning time of the normalization time $T = 1$ was shown in fig. 6.

The removal rate is calculated by weighing the fibrous filter material before and after cleaning, with repeated five times. The removal rate increased from 54.78% to 92.56% when the cleaning flow rate increased from 0.2-1.0 m/s, with an increase of 37.78%. While the removal rate increased from 95.61% when the cleaning flow rate increased from 1.0-2.0 m/s, with an increase of only 3.05%. The final removal rate of particles increases with the increased of cleaning flow rate, but there was a marginal decreasing effect [28].

The distribution of velocity and resistance in the fibrous filter material at the cleaning flow rate was 0.8 m/s, 1.0 m/s, and 1.2 m/s at the normalization time $T = 1$ in fig. 7.

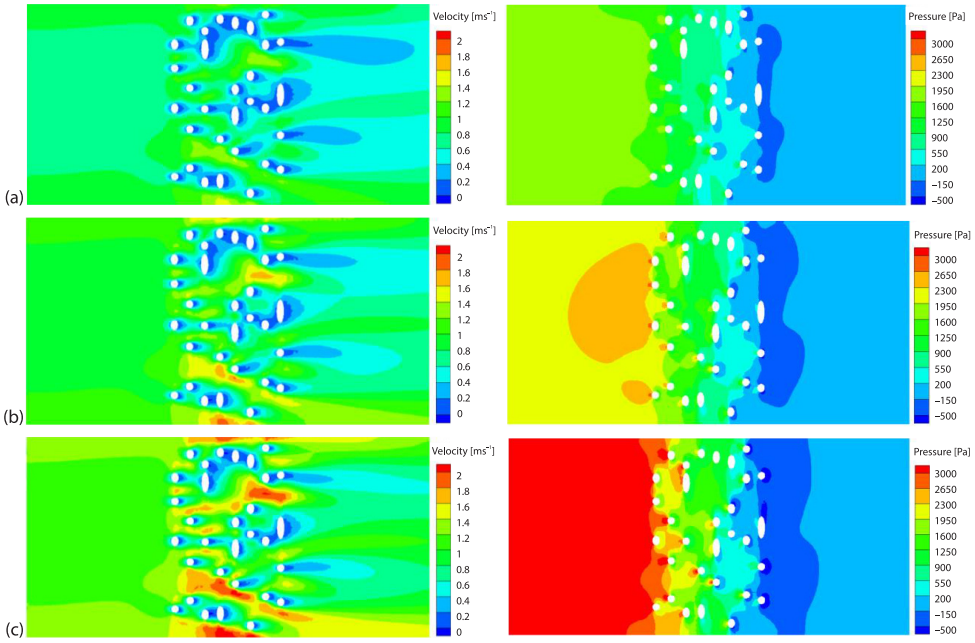

Figure 7. Velocity and resistance distributions of three cleaning velocities; (a) 0.8 m/s, (b) 1.0 m/s, and (c) 1.2 m/s

The presence of the fibers reduced the flow cross-sectional area when the water flowed through the fibers, and the average flow rate of the pores increased by to 40% compared with

the inlet flow rate. The back of the fibers produced low flow rate area, which was also a low resistance area around the fibers. The front row of fibers shaded the back row of fibers so that the resistance decreases layer by layer. The cleaning flow rate increased from 1.0-1.2 m/s, and the average flow rate in the low flow rate region was only increased by 0.02 m/s. The change in flow traction was small and the residual particles were also hardly moved, which explained the small increase in the final removal rate after the cleaning flow rate of 1.0 m/s.

Effect of the cleaning time

The resuspension rate of particles of the surface was increased with the time of the exposure to the fluid [31]. It would reach a constant state only after a period of time. The evolution of the particle removal rate with the normalization time for five different cleaning flow rates was shown in fig. 8(a). The removal rate increased rapidly to 90.63% under the normalization time from 0 to 0.6 at the cleaning flow rate of 1.2 m/s. The removal rate increased slowly under the normalization time from 0.6-0.9, only 2.49%. Figure 8(a) also showed that the particle removal rate are above 80% under the rapid cleaning to stabilization. Comparison of cleaning flow rate 1.2 m/s, 1.6 m/s, and 2.0 m/s, respectively, and $T = 0.6$, 0.4, and 0.2 began to stabilize. The cleaning time had an effect on the regeneration of filter material cleaning effect in a certain range, and then the removal rate tended to stabilize. The higher the cleaning flow rate, the shorter the time to reach stability. The cleaning flow rate was 0.4 m/s and 0.8 m/s, the removal rate for G4 was still not 90% for a longer time. The cleaning flow rate was 1.2 m/s, 1.6 m/s, and 2.0 m/s, and the removal rate reached about 90%, when $T = 0.6$, 0.44, 0.16, respectively. From the engineering considerations, it was not recommended too high flow rate for the requirement of efficient cleaning, which may damage the structure and reduce the life of the filter. The cleaning time corresponding to $T = 0.6$ at 1.2 m/s was 30 seconds, and the fast cleaning to 90.63% removal rate can meet the requirement of reuse. It was suggested that the cleaning parameter for G4 is 1.2 m/s and the flow rate cleaning was 30 seconds. After converting the cleaning time, the fitted surface was shown in fig 8(b). The R^2 was 0.975, which had good coincidence. The relationship between the removal rate and the cleaning flow rate and time for G4 filter material was obtained:

$$E(v,t) = 1.1 - 0.29\mathrm{e}^{-0.48v} - 0.81\mathrm{e}^{-0.11vt},\ (v < 2.1, t > 0) \tag{6}$$

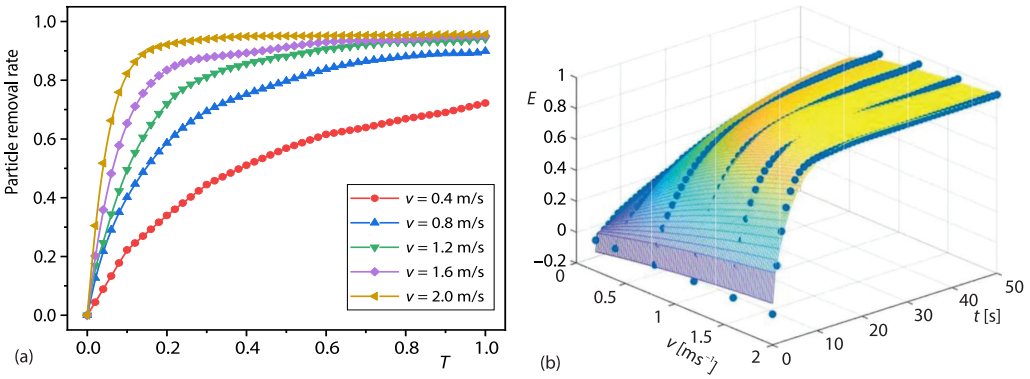

Figure 8. Effect of non-dimensional time on particle removal rate; (a) five different cleaning velocities and (b) fitting surface

Figure 9 shows that the changes of particle dynamics at a position on the windward side, when $T = 0.6$, 0.7, 0.8, 0.9, respectively. The position of the particles on the fiber was

changed, but most of them were not detached, and the velocity gradually stabilizes, only a few particles were resuspension. This may be the particles were continuously disturbed by the fluid in the low speed turbulent environment, the potential energy gradually accumulated, and they will be resuspended when they break through the *potential energy well* of surface adhesion [32]. The energy balanced model [33] can explain this phenomenon to some extent.

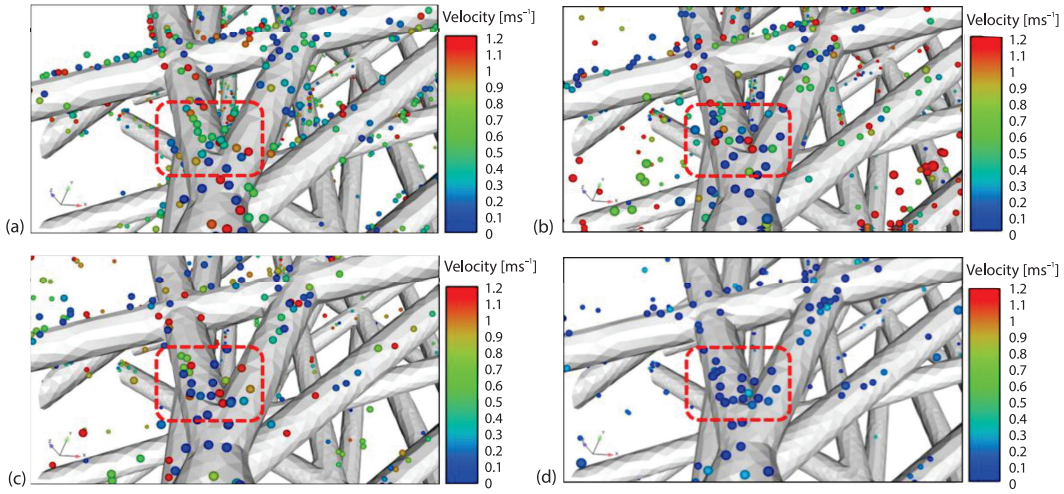

Figure 9. Distribution of particle deposition after different times of cleaning; (a) $T = 0.6$, (b) $T = 0.7$, (c) $T = 0.8$, and (d) $T = 0.9$

Effect of the adhesion force

Figure 10(a) shows that the fiber surface energy γ_f increased from 0.1-0.5 J/m^2 at the particle surface energy of 0.1 J/m^2, and the removal rate decreased from 91.89-80.96% at the cleaning flow rate of 0.8 m/s. This was because the increase of the surface energy of the fibers, which increased the adhesion between the particles and the fibers, and the particles was more difficult to remove from the fibers. Figure 10(b) shows that the γ_p increased from 0.1-0.5 J/m^2 at the γ_f of 0.2 J/m^2, and the removal rate decreased from 89.67-82.72%, which showed the same pattern as fig. 10(a). But the difference was that with the increased in particle surface energy, which was not only increased the adhesion between particles and fibers, but also

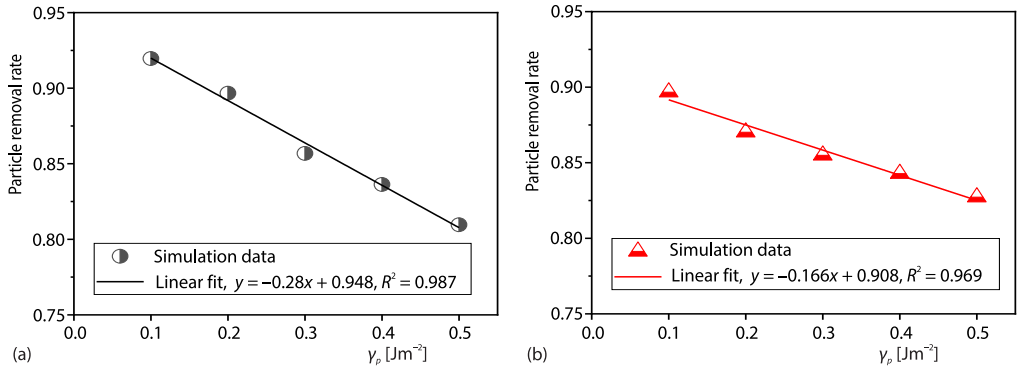

Figure 10. Effect of surface energy; (a) γ_f and (b) γ_p

enhanced the agglomeration of particles. The absolute value of the slope of removal rate of fiber surface energy was 0.28 after linear fitting, which was larger than the absolute value of the slope of removal rate with particle surface energy 0.166. The fiber surface energy played a dominant role in the cleaning process, and reducing the surface energy of fibers can effectively enhance the cleaning and regeneration performance.

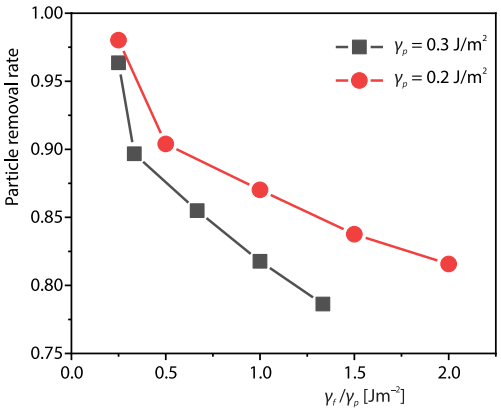

Figure 11. Effect of ratio of surface energy γ_f/γ_p

Figure 11 shows that the variation of particle removal rate with surface energy ratio (γ_f/γ_p) at the cleaning flow rate of 0.8 m/s under the particle surface energy of 0.2 J/m^2 and 0.3 J/m^2, respectively. The removal rate increased significantly from 90.39-98.02% after the ratio was reduced to 0.25 for a particle surface energy of 0.2 J/m^2. The removal rate increased significantly from 89.67-96.36% after reducing the ratio to 0.25 for a particle surface energy of 0.3 J/m^2. The change of γ_f/γ_p at 1/4 is due to the fact that when the surface energy of the particle is constant, which will reduce the surface energy of the fiber reduces the adhesion between the particle and the fiber. Particles deposited in the low velocity region were resuspended under the lower fluid drag, and detached from the fibers.

The results shows a certain cleaning flow rate, the particle removal rate could be improved when the surface energy of the fiber is reduced to 1/4 of the particle surface energy.

Conclusion

The CFD-DEM coupling method was applied to study the water cleaning process of fibrous filter material in this paper. The conclusions of this study can be summarized as following. The removal rate of particles is increased with the increasing of cleaning flow rate, but there was a marginal decreasing effect. For G4 filter material, the best cleaning flow rate was 1.2 m/s, while the cleaning time was 30 seconds. More than 80% of the particles were removed in the initial period in the water cleaning process, and then tended to stabilize. The higher the flow rate, the shorter the time required to reach stability. The surface energy of the fibers plays a dominant role in the process of cleaning. The particle removal rate could be significantly improved when the surface energy of the fiber is reduced to 1/4 of the particle surface energy at a certain cleaning flow rate.

The CFD-DEM method can be used to predict the optimization of cleaning operation parameters and provide guidance about the design of new washable filters.

Acknowledgment

The work was supported by the National Key R and D Program of China (No. 2016YFC0700503) and the Key Research and Development Program of Shaanxi Province of China (No. 2023-YBGY-137), supported by XAUAT Engineering Technology Co., Ltd. (No. XAJD-YF23N003) and the Internal scientific research project of Shaanxi Provincial Land Engineering Construction Group (No. DJNY-YB-2023-13), as well as the College Students' Innovative Entrepreneurial Training Plan Program (No. 202210703024), and the National Natural Science Foundation of China (No. 50806055).

Contribution

Authors Xin Zhang and Zeming Fu equally contributed to this work.

References

[1] Zhang, X., *et al*., Research on Outdoor Design PM2.5 Concentration for Fresh Air Filtration Systems Based on Mathematical Inductions, *Journal of Building Engineering*, *34* (2021), 101883
[2] Bian, Y., *et al*., Influence of Fiber Diameter, Filter Thickness, and Packing Density on PM2.5 Removal Efficiency of Electrospun Nanofiber Air Filters for Indoor Applications, *Building and Environment*, *170* (2020), 106628
[3] Tian, X., *et al*., Effect of main-Stage Filter Media Selection on The Loading Performance of a Two-Stage Filtration System, *Building and Environment*, *195* (2021), 107745
[4] Zhang, X., *et al*., Experimental Study on the Structure and Properties of Modified Non-Woven Filter Fibers by Impregnation with Carbon Black, *Journal of Engineered Fibers and Fabrics*, *15* (2020), Apr., pp. 1-7
[5] Matela, D., Air Filtration: Green and Clean – How to Improve Indoor Air Quality, *Filtration and Separation*, *43* (2006), 9, pp. 24-27
[6] Min, K., *et a*l., Silk Protein Nanofibers for Highly Efficient, Eco-Friendly, Optically Translucent, and Multifunctional Air Filters, *Scientific Reports*, *8* (2018), 1, pp. 1-10
[7] Liu, X. P., *et al*., Effect of Water Cleaning on Performance of Air Filtration Medias, *Advanced Materials Research*, *716* (2013), July, pp. 475-481
[8] Stahl, S., *et al*., The Cleanability of Particle Loaded Woven Filter Media in Solid-Liquid Separation, *Separation and Purification Technology*, *110* (2013), June, pp. 196-201
[9] Weidemann, C., *et al*., Removal Mechanisms of Particulate Contaminations from Polymer Woven Filter Media, *Separation and Purification Technology*, *136* (2014), Nov., pp. 168-176
[10] Baylis, J. R., Review of Filter Bed Design and Methods of Washing, *Journal (American Water Works Association)*, *51* (1959), 11 pp. 1433-1454
[11] Van Staden, S. J., Haarhoff, J., Effective Filter Backwashing with Multiple Washes of Air and Water, *Proceedings*, 9th WISA Biennial Conference, Durban, South Africa, 2006, pp. 22-24
[12] Zhou, Q. M., *et al.*, Spatiotemporal Distribution of Opportunistic Pathogens and Microbial Community in Centralized Rural Drinking Water: One Year Survey in China, *Environmental Research*, *218* (2023), 115045
[13] Wu, S., *et al*., Research Progress on the Cleaning and Regeneration of PM2.5 Filter Media, *Particuology*, *57* (2021), Aug., pp. 28-44
[14] Bai, Y., *et al*., Washable Multilayer Triboelectric Air Filter for Efficient Particulate Matter PM2.5 Removal, *Advanced Functional Materials*, *28* (2018), 15, 1706680
[15] Bowling, R. A., A Theoretical Review of Particle Adhesion, *Particles on Surfaces*, *1* (1988), pp. 129-142
[16] Sheng, Y., *et al*., Analysis of *Filtration Process of 3-D Mesh Spacer Filter by Using CFD-DEM Simulation, Powder Technology, 396* (2022), Part B, pp. 785-793
[17] Qian, F., *et al*., Numerical Study of The Gas-Solid Flow Characteristic of Fibrous Media Based on SEM Using CFD–DEM, *Powder Technology*, *24*9 (2013), Nov., pp. 63-70
[18] Yao, L., *et al*., An Optimized CFD-DEM Method for Fluid-Particle Coupling Dynamics Analysis, *International Journal of Mechanical Sciences*, *174* (2020), 105503
[19] Di, R. A., Maio, F. P. D., Comparison of contact-Force Models for the Simulation of Collisions in DEM-Based Granular Flow Codes, Chemical Engineering Science, *59* (2004), 3, pp. 525-541
[20] Maugis, D., Adhesion of Spheres: The JKR-DMT Transition Using a Dugdale Model, *Journal of Colloid* and Interface Science, *150* (1992), 1, pp. 243-269
[21] Henry, C., Minier, J. P., Progress in particle Resuspension from Rough Surfaces by Turbulent Flows, *Progress in Energy and Combustion Science*, *45* (2014), Dec., pp. 1-53
[22] Xie, J., *et al*., MP-PIC Modelling of CFB Risers with Homogeneous and Heterogeneous Drag Models, *Advanced Powder Technology*, *29* (2018), 11, pp. 2859-2871
[23] Yue, C.,. *et al*., Numerical Simulation of the Filtration Process in Fibrous Filters Using CFD-DEM Method, *Journal of Aerosol Science*, *101* (2016), Nov., pp. 174-187
[24] Cao, B., *et al*., Pressure Drop Model for Fibrous Media in Depth Filtration: Coupling Simulation of Microstructure and CFD Porous Media during Dust Loading, *Building and Environment*, *202* (2021), 108015
[25] Liu, H., *et al*., Progress on Particulate Matter Filtration Technology: Basic Concepts, Advanced Materials, and Performances, *Nanoscale*, *12* (2020), 2, pp. 437-453

[26] Li, H., *et al*., Turbulence Model Selection and Flow Field Analysis of the Micro Irrigation Screen Filter Based on Porous Medium Using CFD, *Journal of Irrigation and Drainage*, *35* (2016), 4, pp. 14-19
[27] Cheng, K., *et al.*, The CFD-DEM Simulation of Particle Deposition Characteristics of Pleated Air Filter Media Based on Porous Media Model, *Particuology*, *72* (2023), 4, pp. 37-48
[28] Qian, F. P., *et al*., The CFD-DEM Simulation of the Filtration Performance for Fibrous Media Based on the Mimic Structure, *Computers and Chemical Engineering*, *71* (2014), Dec., pp. 478-488
[29] Zhang, X., *et al*., Influence of Fiber Diameter on Filtration Performance of Polyester Fibers, *Thermal Science*, *23* (2019), 4, pp. 2291-2296
[30] Jackson, G. W., James, D. F., The Permeability of Fibrous Porous Media, *The Canadian Journal of Chemical Engineering*, *64* (1986), 3, pp. 364-374
[31] Ziskind, G., *et a*l., Resuspension of Particulates from Surfaces to Turbulent Flows – Review and Analysis, *Journal of Aerosol Science*, *26* (1995), 4, pp. 613-644
[32] Stempniewicz, M. M., *et al*., Model of Particle Resuspension in Turbulent Flows, *Nuclear Engineering and Design*, *238* (2008), 11, pp. 2943-2959
[33] Vainshtein, P., *et al*., Kinetic Model of Particle Resuspension by Drag Force, *Physical Review Letters*, *78* (1997), 3, pp. 551-554

Paper submitted: February 2, 2023
Paper revised: March 5, 2023
Paper accepted: March 7, 2023